

Copyright © 1985, by the author(s).  
All rights reserved.

Permission to make digital or hard copies of all or part of this work for personal or classroom use is granted without fee provided that copies are not made or distributed for profit or commercial advantage and that copies bear this notice and the full citation on the first page. To copy otherwise, to republish, to post on servers or to redistribute to lists, requires prior specific permission.

DEVIL'S STAIRCASE ROUTE TO CHAOS  
IN A NONLINEAR CIRCUIT

by

L. O. Chua, Y. Yao and Q. Yang

Memorandum No. UCB/ERL 85/98

6 December 1985

COVER PAGE

DEVIL'S STAIRCASE ROUTE TO CHAOS  
IN A NONLINEAR CIRCUIT

by

L. O. Chua, Y. Yao and Q. Yang

Memorandum No. UCB/ERL 85/98

6 December 1985

ELECTRONICS RESEARCH LABORATORY

College of Engineering  
University of California, Berkeley  
94720

TITLE PAGE

RUN BLANK BACK

DEVIL'S STAIRCASE ROUTE TO CHAOS  
IN A NONLINEAR CIRCUIT<sup>1</sup>

L.O. Chua, Y. Yao and Q. Yang<sup>2</sup>

*ABSTRACT*

A driven 2nd-order negative-resistance oscillator circuit has been observed experimentally to exhibit infinitely many distinct chaotic states in addition to infinitely many subharmonic responses of all orders. Each chaotic state is found to be born out of a devil's staircase whose steps are spaced in accordance with a definite *period-adding law*.

Each devil's staircase emerges at some level of frequency-tuning resolution, where each level is embedded within an outer level, *ad infinitum*. The global bifurcation structure is *self-similar* in the sense that upon rescaling, the devil's staircases appear to be clones of each other.

---

<sup>1</sup>This research is supported in part by the Office of Naval Research under Contract N00014-70-C-0572 and by the National Science Foundation under Grant ECS-8313278.

<sup>2</sup>L.O. Chua is with the University of California, Berkeley. Y. Yao and Q. Yang are with the Shanghai Jiao Tong University, Shanghai, China.

## 1. INTRODUCTION

It is now well known that *chaos* can occur in a 2nd-order non-autonomous circuit [1-2] via a *period-doubling route* [3-5]. Another possible route to chaos, called the *period-adding route*, was recently observed in a 1-dimensional nonlinear *discrete map* by Kaneko [6-8]. Our objective in this paper is to report a detailed *experimental* study which shows that the period-adding route to chaos can also occur in a nonlinear circuit described by *ordinary differential equations*.

Our circuit essentially consists of a 2nd-order negative-resistance oscillator driven by a sinusoidal voltage source. By varying the *frequency*  $f_s$  of this voltage source while holding all other parameters fixed, we observe a very intricate sequence of bifurcation phenomena. In particular, subharmonics of *all orders* are found to occur over a wide range of the input frequency. Sandwiched between every pair of subharmonics is a *chaotic* response which is born out of a period-adding sequence.

More careful measurements reveal a fascinating patterns of *self-similar* bifurcation structures, each resembling a *devil's staircase* [9]. Between every two adjacent steps of each devil's staircase we find a miniature version of another devil's staircase, whose adjacent steps themselves harbor even smaller miniaturized devil's staircases. In other words, as we increase the resolution of our frequency tuning experiments, we keep discovering more miniaturized versions of period-adding routes to chaos. At a given level of resolution, the associated devil's staircase appears as an ascending series of steps where the spacing between them varies according to a simple law. As one climbs up the steps in any of these infinitely many devil's staircases, the *width* (i.e., the frequency interval  $\Delta f_s$ , where the subharmonic response corresponding to each step can be observed) of the steps decreases rapidly until chaos sets in.

Since the above bifurcation phenomenon has been observed at every level of resolution of our measuring instruments, we conjecture that all *chaotic states* in this circuit — and there are infinitely many of them — are born out of self-similar devil's staircases of

which there are infinitely many.

To clarify the above rather bizarre bifurcation phenomena, we have included a large collection of bifurcation diagrams and Lissajous figures in this paper. Readers unfamiliar with the devil's staircase may wish to glance first at Figs. 6, 8, 10, 11 and 13, each of which harbors a devil's staircase belonging to the next level.

One main goal of this paper is to provide the full experimental details of the above cited devil's staircase routes to chaos and to formulate an empirical law which can be used to predict the spacings between steps in each devil's staircase at any level of frequency tuning resolution.

## 2. EXPERIMENTAL CIRCUIT AND MEASUREMENT PROCEDURE

The circuit used in our experiment is shown in Fig.1 where the *nonlinear* resistor is a type-S negative resistance device synthesized by the 2-transistor circuit shown in Fig.2(a) [10]. Its measured  $v_R - i_R$  characteristic is shown in Fig.2(b). Our basic experimental procedure consists of adjusting the frequency  $f_s \triangleq \omega_s / 2\pi$  of our sinusoidal signal generator (with all other parameters held fixed) while carrying out the following measurement tasks:

1. Determine whether the capacitor voltage waveform  $v_c(t)$  is *periodic* or not for each frequency setting  $f_s$ .
2. If  $v_c(t)$  is found to be periodic, determine its period  $T_c$ . Since all periodic wave forms that we have observed from this circuit are *subharmonics* of the input signal with periods  $T_c = nT_s$ , where  $T_s = \frac{1}{f_s}$  and  $n$  is an integer, we will report our results in terms of the *normalized period*  $P \triangleq \frac{T_c}{T_s} = n$ .

For the circuit in Fig.1, we have found from our experiments that both the periodicity and the normalized period  $P$  of  $v_c(t)$  can be efficiently and reliably determined by tracing the Lissajous figure [11] associated with the capacitor voltage waveform  $v_c(t)$  and

the resistor-voltage source waveform  $v_s(t)$  in the oscilloscope. In the Appendix, we proved that  $v_c$  and  $v_s$  are related by the 2nd order non-autonomous state equation

$$\begin{aligned}\dot{v}_c &= f_1(v_c, v_s, t) \\ \dot{v}_s &= f_2(v_c, v_s, t)\end{aligned}\tag{1}$$

Choosing  $v_c$  and  $v_s$  rather than the more conventional  $v_c$  and  $i_L$  as state variables in our Lissajous figure allows us to ascertain not only the periodicity of  $v_c(t)$  but also its normalized period  $P$  in a single measurement: The Lissajous figure is a closed loop if and only if both  $v_c(t)$  and  $v_s(t)$  are periodic with commensurable periods (i.e., their ratio is a rational number). Moreover, since the waveform of

$$v_s(t) = E \cos \omega_s t - R_s C \dot{v}_c(t)\tag{3}$$

contains the same number "n" of wave crests as that of the the input signal  $E \cos \omega_s t$  over each period  $T_c = nT_s$  of  $v_c(t)$ , we can identify "n" by simply counting the number of corresponding "crests on the left side"<sup>3</sup> of the Lissajous figure generated by  $v_s(t)$  (applied to horizontal channel).

For example, the Lissajous figure in Fig.3(a), (c), and (e) has 3, 5 and 23 crests on its left side, respectively, and hence  $n=3$ , 5, and 23, respectively.

It is often useful to relate the shape of the Lissajous figure with some basic features of either  $v_s(t)$  or  $v_c(t)$ . For example, the *lower* waveform in Figs.3(b) and (d) denotes  $v_s(t)$  while that in Fig.3(f) denotes  $v_c(t)$  used in tracing the Lissajous figure in Fig.3(a), (c), and (e), respectively. For time reference purposes, the sinusoidal input signal is taken at the same time interval and is aligned on top of each of these waveforms. Note that  $v_s(t)$  has 3 wave crests per period in Fig.3(b) and 5 wave crests per period in Fig.3(d). Since  $v_s(t)$  is applied to the horizontal channel, the Lissajous figure in Fig.3(a) and (c) must exhibit 3 and 5 crests on the left side, respectively, similarly, since  $v_c(t)$  has only one local maximum and one local minimum per period in Fig.3(f), and since it is applied to

---

<sup>3</sup> A "crest on the left side" of a Lissajous figure is defined to be a local maximum when the Lissajous figure is rotated by  $90^\circ$  in the clock wise direction.

the vertical channel, it follows that the Lissajous figure in Fig.3(e) can traverse only once upward and once downward while swinging left and right a total of 12 times.

As examination of Fig.3(f) shows that while it is difficult to count the order "n" of the subharmonics from the waveforms when n is large (n=23 in this case), it is much easier to identify n from its associated Lissajous figure in Fig.3(e). Note also that had we applied the input signal, instead of  $v_s(t)$ , to the horizontal channel, the resulting Lissajous figure would have intertwined itself many times that once again it would be difficult to identify n accurately. Our choice of  $v_s(t)$  has therefore the effect of spreading out the loci traversed by the Lissajous figure so that the number of crests on the left can be easily identified even for fairly large n.

### 3. EXPERIMENTAL RESULTS

As we decrease the frequency  $f_s$  from 20 kHz to 500 Hz, with all other parameters held fixed, we observe subharmonics of all orders from 2 to 33. Each subharmonic is found to persist over a limited range of the input frequency  $f_s$ , thereby creating a step-like bifurcation diagram where the normalized period P is plotted as a function of  $f_s$ . Each step in this diagram can be interpreted as a synchronization state between the input frequency and some submultiple of the circuit's *natural* frequency; i.e., the oscillation frequency when the input signal is set to zero. The length of each step can therefore be interpreted as the "locking range". While some steps are rather wide (e.g., 300 Hz) and easily reproduced, others are so narrow that the step reduces to a point within the resolution of our measurement instruments.

Each pair of adjacent steps is separated by a narrow "frequency gap" where *chaos* is observed at some frequency within the gap. A more careful tuning within each gap reveals an extremely rich dynamical structure: for each finer level of tuning resolution, a new step-like structure called a *devil's staircase* emerges. In the following subsections, we summarize the experimental results at each level of resolution and derive an empirical law

governing the spacing between the steps.

*A. Level 1 Devil's Staircase*

The bifurcation diagram of  $P$  vs.  $f_s$ , which we observed at the *lowest* level of resolution consists of a uniform succession of steps from 1 to 33 as shown in Fig.4. For reasons that will be obvious soon, we call this structure a level-1 devil's staircase [9]. The steps are separated by narrow gaps whose width is assumed to be zero at this level of frequency resolution: i.e., each tuning frequency increment  $(\Delta f)_1$  is larger than the widest gap in Fig.4. Following Kaneko [6], we call this bifurcation phenomenon a "period-adding bifurcation" because the normalized period of each new subharmonic waveform is obtained by *adding* the normalized input period 1 to the period before bifurcation. This is fundamentally different from the well-known "period-doubling" bifurcation [5] where the steps occur at 1, 2, 4, 8, 16, 32, ... etc., instead of 1, 2, 3, 4, 5, 6, 7, 8, ..., etc. in Fig.4.

The Lissajous figures corresponding to several steps in Fig.4 are shown in Fig.5 along with their associated waveforms  $v_s(t)$  and  $v_c(t)$  (shown below the input reference sinusoidal signal). In particular, a period-15 Lissajous figure is shown in Fig.5(a), a period-10 Lissajous figure is shown in Fig.5(d), a period-8 Lissajous figure is shown in Fig.5(g), a period-3 Lissajous figure is shown in Fig.5(j), and a period-2 Lissajous figure is shown in Fig.5(m). The two waveforms  $v_s(t)$  and  $v_c(t)$  are shown directly below their associated Lissajous figures in the order listed.

We will summarize our above observations as follows:

*level-1 devil's staircase sequence from step 33 to step 1*

$$\dots \rightarrow 33 \rightarrow 32 \rightarrow 31 \rightarrow 30 \rightarrow \rightarrow \dots \rightarrow 5 \rightarrow 4 \rightarrow 3 \rightarrow 2 \rightarrow 1 \quad (4)$$

The spacing between the *broken* arrow head denotes the "gap" whose structure we will investigate next.

*B. Level-2 Devil's Staircase*

Let us now increase the resolution of our frequency tuning experiment by decreasing the frequency increment (say  $(\Delta f)_2 = 0.1 (\Delta f)_1$ ) so that the frequency gap between each pair of adjacent steps in Fig.4 is magnified sufficiently to reveal some (but not all!) finer structures.

The magnification of the "gap" between 1 and 2 is shown in Fig.6. As we decrease  $f_s$  from about 850 Hz, we discover a new family of steps whose order increases consecutively from step 2 to 3, to 4, to 5, .... etc., *ad infinitum*,<sup>4</sup> and finally to a *chaotic* state before descending back to the left boundary of the *period-1* step at around 640 Hz.

The Lissajous figures corresponding to several steps in Fig.6 are shown in Fig.7 along with their associated waveforms  $v_s(t)$  and  $v_c(t)$  as in Fig.5. In particular, the Lissajous figures corresponding to a period 2, 3, 4, 5, 6, 7, and 8 periodic states are shown in Figs. 7(a), (d), (g), (j), (m), (p), and (s), respectively. The Lissajous figure in Fig.7(v) never closes upon itself and corresponds to a *chaotic* state.

As we further decrease  $f_s$  to the left boundary of the gap, the chaotic waveform  $v_c(t)$  suddenly collapses and reverts back to a periodic waveform of period 1 whose Lissajous figure is shown in Fig.7(w).

Further tuning resolution will soon reveal that every 2 steps within the gap in Fig.6 are in turn separated by narrower gaps whose widths are all assumed to be zero at our level-2 resolution. We call this ascending sequence of steps within the gap in Fig.6 a *level-2 devil's staircase* [9]. Hence, as we decrease  $f_s$  from 850 Hz to 640 Hz, we climb up the level-2 devil's staircase to an arbitrarily high step before plunging down to a period-1 periodic state. We will henceforth refer to this scenario, as well as similar scenarios below, as the devil's staircase route to chaos.

---

<sup>4</sup> Clearly, our finite instrument resolution allows us to identify only the first few steps in this sequence. It appears, however, that this sequence continues *ad infinitum* following a definite law to be determined in the next section.

Let us summarize Fig.6 as follows:

*level-2 devil's staircase sequence from step 2 to step 1*

$$2 \rightarrow 3 \rightarrow 4 \rightarrow 5 \rightarrow 6 \rightarrow 7 \rightarrow 8 \rightarrow \dots \rightarrow \text{chaos} \rightarrow 1 \quad (5)$$

The magnification of the "gap" between steps 2 and 3 is shown in Fig.8. As we decrease the frequency  $f_s$  from above 1300 Hz, we discover again a new family of steps whose period increases from 3 to 5, to 7, to 9, .... etc., *ad infinitum*, and finally to a *chaotic* state before descending back to the left boundary of the *period-2* step at around 1100 Hz.

The Lissajous figures corresponding to several steps in Fig.8 are shown in Fig.9 along with their associated waveforms  $v_s(t)$  and  $v_c(t)$  as in Fig.5. In particular, the Lissajous figures corresponding to a period 3, 5, 7, 9, 11, and 13 periodic states are shown in Figs.9(a), (d), (g), (j), (m) and (p), respectively. The Lissajous figure in Fig.9(s) never closes upon itself and correspond to a *chaotic state*.

As we further decrease  $f_s$  to the left boundary of the gap, the chaotic wave form  $v_c(t)$  suddenly collapses and reverts back to a periodic wave form of period 2 whose Lissajous figure is shown in Fig.9(u).

Hence, just as in Fig.6, we have here a devil's staircase route to chaos.

Let us summarize Fig.8 as follows:

*level-2 devil's staircase sequence from step 3 to step 2*

$$3 \rightarrow 5 \rightarrow 7 \rightarrow 9 \rightarrow 11 \rightarrow 13 \rightarrow \dots \rightarrow \text{chaos} \rightarrow 2 \quad (6)$$

The magnification of the "gap" between steps 3 and 4 is shown in Fig.10. As we decrease the frequency  $f_s$  from about 1840 Hz, we discover a similar devil's staircase route to chaos, which we summarize as follows:

*level-2 devil's staircase sequence from step 4 to step 3*

$$4 \rightarrow 7 \rightarrow 10 \rightarrow 13 \rightarrow 16 \rightarrow \dots \rightarrow \text{chaos} \rightarrow 3 \quad (7)$$

Indeed, the same scenarios have been observed in every gap in Fig.4 which we have measured. From these observations, we can deduce the following empirical law which defines

the

*level-2 devil's staircase sequence from step n+1 to step n*

$$(n+1) \rightarrow (n+1)+n \rightarrow (n+1)+2n \rightarrow (n+1)+3n \rightarrow (n+1)+4n \\ \rightarrow \dots \rightarrow \text{chaos} \rightarrow n \quad (8)$$

As a check, note that if we let  $n=1, 2,$  and  $3,$  respectively, in (8), we could obtain (5), (6), and (7), respectively.

### C. Level-3 Devil's Staircase

Let us now increase the resolution of our frequency tuning experiment even further (say  $(\Delta f)_3 = 0.1 (\Delta f)_2 = 0.01 (\Delta f)_1$ ) so that the frequency gap between each pair of adjacent steps in Figs.6, 8 and 10 is magnified further to reveal additional (but not all!) yet finer structures.

The magnification of the "gap" between steps 2 and 3 in Fig.6 is shown in Fig.11. As we decrease the frequency  $f_s$  from about 860 Hz, we discover yet another family of devil's staircase as shown in Fig.11, which increases from step 2 to 5, to 8, to 11, ... etc., *ad infinitum*, and finally to yet another *chaotic* state before plunging back to the left boundary of the *period-3* step at around 780 Hz. Hence, once again, we observe a devil's staircase route to chaos.

The Lissajous figures corresponding to several steps in Fig.11 are shown in Fig.12. In particular, the Lissajous figures corresponding to a period 2, 5 and 8 periodic states are shown in Fig.12(a), (b) and (c), respectively. The Lissajous figure in Fig.12(d) never closes upon itself and corresponds to a *chaotic state*. The Lissajous figure in Fig.12(e) corresponds to the period-3 periodic state right after chaos.

For comparison purposes, the waveforms  $v_s(t)$  and  $v_c(t)$  associated with the period-5 Lissajous figure in Fig.12(b) are shown in Figs.12(f) and (g), respectively.

Let us summarize Fig.11 as follows:

*level-3 devil's staircase sequence from step 2 to step 3*

$$2 \rightarrow 5 \rightarrow 8 \rightarrow 11 \rightarrow 14 \rightarrow 17 \rightarrow \dots \rightarrow \text{chaos} \rightarrow 3 \quad (9)$$

Likewise, the magnification of the "gap" between steps 3 and 5 in Fig.8 is shown in Fig.13. Once again, we see a devil's staircase route to chaos. Figs.14(a) and (b) show the Lissajous figures corresponding to a period-3 and period-8 step in this staircase. The Lissajous figure corresponding to the chaotic state and the final transition to a period-5 periodic state are shown in Figs.14(c) and (d) respectively.

We can summarize Fig.14 as follows:

*level-3 devil's staircase sequence from step 3 to step 5*

$$3 \rightarrow 8 \rightarrow 13 \rightarrow 18 \rightarrow 23 \rightarrow 28 \rightarrow \dots \rightarrow \text{chaos} \rightarrow 5 \quad (10)$$

Repeated experiments at level-3 accuracy for several other gaps in Figs. 6,8, and 10 reveal the following empirical law:

*level-3 devil's staircase sequence from step p to step q*

$$p \rightarrow p+q \rightarrow p+2q \rightarrow p+3q \rightarrow \dots \rightarrow p+nq \dots \rightarrow \text{chaos} \rightarrow q \quad (11)$$

As a check on the validity of this empirical law, observe that if we let  $p=2$  and  $q=3$  in (11), we would obtain (9). Similarly, if we let  $p=3$  and  $q=5$  in (11), we would obtain (10).

In fact, if we let  $p=n+1$  and  $q=n$  in (11), we would obtain the *level-2* empirical law in (8). it appears therefore that the empirical law (11) is quite general, at least for the non-linear circuit in Fig.1, and can be used to predict the sequence of steps in any devil's staircase route to chaos, at any level.

#### *D. Robustness*

To ensure that the above devil's staircase route to chaos is rather robust, we repeated our experiments with different transistors and parameters. In each case, the same qualitative behavior is observed. Fig.15 is a case in point. The Lissajous figures here are

qualitatively similar to the corresponding ones in Fig.9. In particular, Figs.9(a) and 15(a), Figs.9(d) and 15(d), Figs.9(g) and 15(c), Fig.9(j) and 15(d), Figs.9(m) and 15(e), Figs.9(p) and 15(f), Figs.9(s) and 15(g), and finally Figs.9(u) and 15(h), are similar to each other. Yet, these Lissajous figures are traced with a different transistor (NPN type no.3DG 100A) and a different set of parameters ( $E=0.48V$ ,  $E_B=2.45V$ ,  $C=10\mu F$ ).

#### 4. CONCLUSION

Based on extensive experimental observations, we conjecture that the bifurcation phenomena for the nonlinear circuit in Fig.1 (with the input frequency  $f_s$  as the tuning parameter) consists of an infinitely many levels of devil's staircases, each one having a finer resolution than its preceding level. The ascending steps in each devil's staircase are sandwiched between 2 adjacent steps which themselves belong to another devil's staircase at level (k-1). The steps belonging to each devil's staircase at any level k obeys the following *period-adding law*:

$$\begin{aligned}
 p &\rightarrow p+q \rightarrow p+2q \rightarrow p+3q \rightarrow \dots \rightarrow p+nq \rightarrow p+(n+1)q \\
 &\rightarrow \dots \rightarrow \text{chaos} \rightarrow q
 \end{aligned} \tag{12}$$

This "period-adding law" is distinctly different from the well-known "period-doubling law" discovered by Feigenbaum [3]. It is similar, however, to the phenomenon first discovered by Kaneko for nonlinear *discrete* maps [6-8].

A careful analysis of the level-1 devil's staircase in Fig.4 shows that each *step*  $P=n$  always occurs in the vicinity of  $f_s = nf_0$ , where  $f_0 \approx 500 \text{ Hz}$  is the circuit's *natural* frequency measured with the voltage source short circuited. For example, the  $n=5$  step occurs in the vicinity of  $5(500)=2500 \text{ Hz}$  while the  $n=26$  step occurs in the vicinity of  $26(500)=13000 \text{ Hz}$ . We can therefore interpret each step in Fig.4 as a *synchronization* between the input frequency  $f_s$  and some multiple of the natural frequency  $f_0$ .

A similar analysis of the higher-level staircases in Figs.6, 8, 10, 11, and 13 reveals that each  $P=n$  step in a level-k devil's staircase occurs in the vicinity of  $f_s = (\frac{n}{k})f_0$ . For

example, the  $n=3$  step in the level-2 devil's staircase in Fig.6 occurs in the neighborhood of  $f_s = (\frac{3}{2})500 = 750 \text{ Hz}$ . Likewise, the  $n=5$  step in the level-3 devil's staircase in Fig.11 occurs in the neighborhood of  $f_s = (\frac{5}{3})500 = 833 \text{ Hz}$ . We can therefore interpret each step  $P=n$  in a level- $k$  devil's staircase as a synchronization phenomenon between the  $k$  *th* multiple of the input frequency  $f_s$  and the  $n$  *th* multiple of the circuit's natural frequency.

Finally we remark that *qualitatively* similar bifurcation behaviors have also been observed with other circuit parameters chosen as the bifurcation parameter. We have chosen  $f_s$  as our bifurcation parameter in this paper because  $f_s$  can be more accurately tuned than the other circuit elements.

## APPENDIX

Our objective in this Appendix is to derive the state equations governing the circuit in Fig.1 with  $v_c$  and  $v_s$  chosen as the state variables. The state equation for  $v_c$  can be obtained by inspection:

$$\dot{v}_c = \frac{E \cos \omega_s t - v_s}{CR_s} \triangleq f_1(v_c, v_s, t) \quad (\text{A.1})$$

To derive the state equation for  $v_s$ , differentiate the equation

$$i_L = \frac{E \cos \omega_s t - v_s}{R_s} \quad (\text{A.2})$$

with respect to time and solve for  $\dot{v}_s$  to obtain

$$\dot{v}_s = -R_s \dot{i}_L - E \omega_s \sin \omega_s t \quad (\text{A.3})$$

Solving the equation

$$L \dot{i}_L = v_s - v_c - v_R \quad (\text{A.4})$$

for  $\dot{i}_L$  and substituting the result in (A.3), we obtain

$$\dot{v}_s = -\frac{R_s}{L} \left[ v_s - v_c - v_R \right] - \frac{E}{L} \omega_s \sin \omega_s t \quad (\text{A.5})$$

It remains for us to express  $v_R$  in (A.5) in terms of the state variables  $v_c$  and  $v_s$ . To do this, note that

$$i_R = C \dot{v}_c - \frac{1}{R_B} \left[ f(i_R) - E_B \right] \quad (\text{A.6})$$

Substituting (A.1) for  $\dot{v}_c$  into (A.6) and rearranging the equation, we obtain

$$f(i_R) + R_B i_R = E_B + \frac{R_B}{R_s} \left[ E \cos \omega_s t - v_s \right] \quad (\text{A.7})$$

For any value of  $v_s$  and  $t$ , (A.7) has a *unique* solution

$$i_R = h(v_s, t) \quad (\text{A.8})$$

$$R_B > -f'(i_R) \text{ for all } i_R \quad (\text{A.9})$$

This condition is equivalent to requiring the bias resistance  $R_B$  to be large enough so that its associated load line intersects the  $v_R - i_R$  curve at only one point. Since this is the

same condition for the circuit to function as a negative-resistance oscillator when  $E=0$ , it follows that

$$\dot{v}_s = -\frac{R_s}{L} \left[ v_s - v_c - f \left( h(v_s, t) \right) \right] - \frac{E}{L} \omega_s \sin \omega_s t$$

$$\triangleq f_2(v_c, v_s, t) \tag{A.10}$$

Equations (A.1) and (A.10) are the desired state equations for the circuit in Fig.1.

## FIGURE CAPTIONS

- Fig. 1 A negative-resistance oscillator circuit driven by a sinusoidal voltage source of frequency  $f_s$ . Here,  
 $R_s = 200\Omega$ ,  $R_B = 470\Omega$ ,  $L = 0.1 H$ ,  $C = 7 \mu F$ ,  $E = 1 V$  and  $E_B = 2.6 V$ .
- Fig. 2 (a) A 2-transistor realization of the negative-resistance device in Fig.1. Here,  
 $R_1 = 2.2K \Omega$ ,  $R_2 = 560\Omega$  and  $R_3 = 120\Omega$   
 NPN transistor has type no. 3DG6D.  
 (b)  $v_R - i_R$  characteristic curve of the negative resistance device.
- Fig. 3 (a) A P=3 Lissajous figure.  
 (b) Reference sine wave (top) and 3rd order subharmonic waveform for  $v_s(t)$  (below) applied to horizontal channel.  
 (c) A P=5 Lissajous figure.  
 (d) Reference sine wave (top) and 5th order subharmonic waveform for  $v_s(t)$  (below) applied to horizontal channel.  
 (e) A P=23 Lissajous figure.  
 (f) Reference sine wave (top) and 23rd order subharmonic waveform for  $v_c(t)$  applied to vertical channel.
- Fig. 4 Level-1 devil's staircase. P denotes the order of the subharmonic response relative to the forcing frequency  $f_s$ . Encircled regions are magnified in Figs. 6, 8, and 10 and represent level-2 devil's staircases.
- Fig. 5 Lissajous figures associated with Fig.4 and the waveforms for  $v_s(t)$  and  $v_c(t)$  along with reference sine wave on top of each waveform.  $v_s(t)$  is always applied to the horizontal channel while  $v_c(t)$  is always applied to the vertical channel. Each Lissajous figure is followed by  $v_s(t)$  and then by  $v_c(t)$ .  
 (a),(b),(c) : P=15; (d),(e),(f) : P=10; (g),(h),(i) : P=8;  
 (j),(k),(l) : P=3; (m),(n),(o) : P=2
- Fig. 6 Level-2 devil's staircase between steps 1 and 2: magnification of the gap between steps 1 and 2 in Fig.4. Encircled region is further magnified in Fig.11, giving rise to a level-3 devil's staircase.
- Fig. 7 Lissajous figure associated with Fig.6 and the waveforms for  $v_s(t)$  and  $v_c(t)$ . Interpret as in Fig.5 caption.  
 (a),(b),(c) : P=2; (d),(e),(f) : P=3; (g),(h),(i) : P=4;  
 (j),(k),(l) : P=5; (m),(n),(o) : P=6; (p),(q),(r) : P=7;  
 (s),(t),(u) : P=8  
 (v) chaos (w) : P=1
- Fig. 8 Level-2 devil's staircase between steps 2 and 3: magnification of the gap between steps 2 and 3 in Fig.4. Encircled region is further magnified in Fig.13, giving rise to a level-3 devil's staircase.
- Fig. 9 Lissajous figures associated with Fig.8 and the waveforms for  $v_s(t)$  and  $v_c(t)$ . Interpret as in Fig.5 caption.  
 (a),(b),(c) : P=3; (d),(e),(f) : P=5; (g),(h),(i) : P=7;  
 (j),(k),(l) : P=9; (m),(n),(o) : P=11; (p),(q),(r) : P=13;  
 (s) chaos; (t)  $v_s(t)$  chaotic waveform  
 (u) P=2; (v)  $v_c(t)$  waveform.



## REFERENCES

1. A. Azzouz, R. Duhr and M. Hasler, "Transition to chaos in a simple nonlinear circuit driven by a sinusoidal voltage source", *IEEE Trans. Circuits and Systems*, vol. CAS-30, pp.913-914, Dec. 1983.
2. T. Matsumoto, L.O. Chua and S. Tanaka, "Simplest chaotic nonautonomous circuit", *Physical Review A*, Vol. 30, no. 2, pp. 1155-1157, August 1984.
3. M.J. Feigenbaum, "Quantitative universality for a class of nonlinear transformations", *J. Statistical Physics*, vol.19, pp.25-52, 1978.
4. J. Guckenheimer and P. Holmes, *Nonlinear oscillations, dynamical systems and bifurcations of vector fields*, Springer-Verlag, New York, 1983.
5. P. Cvitanovic, *Universality in chaos*, Adam Hilger Ltd., Bristol, 1984.
6. K. Kaneko, "On the period-adding phenomena at the frequency locking in a one-dimensional mapping", *Progress Theoretical Physics* vol.68, no.2, pp.669-672, August 1982.
7. K. Kaneko, "Similarity structure and scaling property of the period-adding phenomena", *Progress of Theoretical Physics*, vol.69, no.2, pp.403-414, February 1983.
8. K. Kaneko, "Transition from torus to chaos accompanied by frequency lockings with symmetry breaking", *Progress of Theoretical Physics*, vol.69, no.5, pp.1427-1442, May 1983.
9. B.B. Mandelbrot, *The fractal geometry of nature*, W.H. Freeman and Company, New York, 1983.
10. L.O. Chua, J.B. Yu and Y.Y. Yu, "Negative resistance devices", *International Journal of Circuit Theory and Applications*, vol.11, pp.161-186, April, 1983.
11. J. Haag, *Oscillatory Motions*, Wadsworth Publishing Co. Belmont, California 1962.

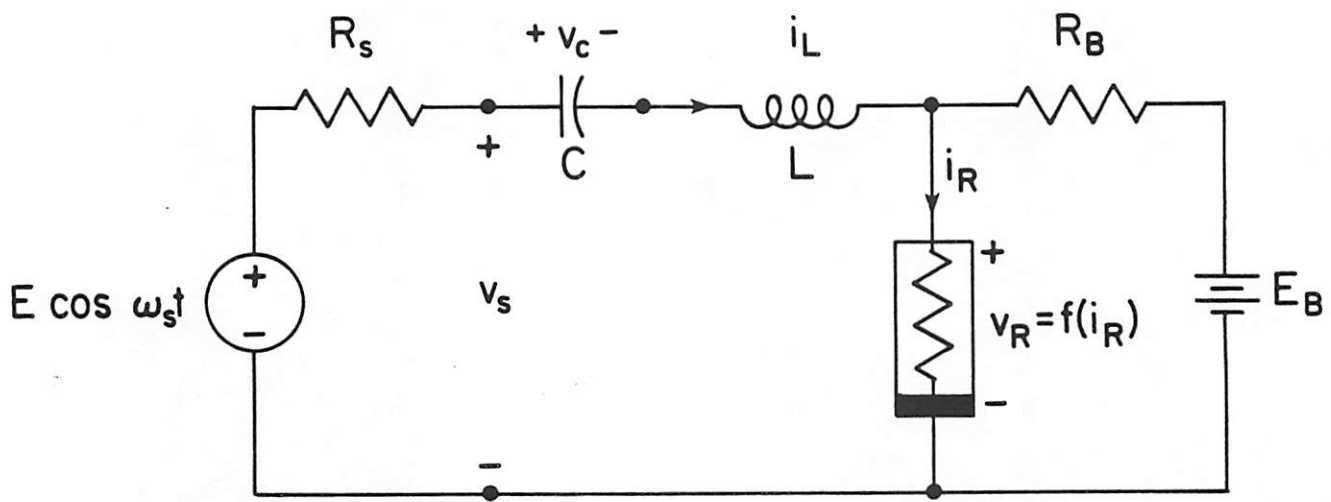
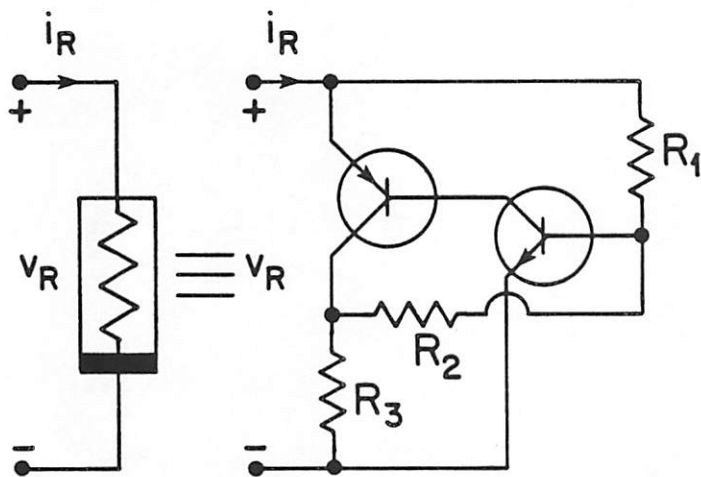
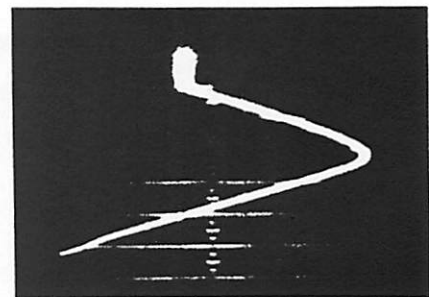


Figure 1

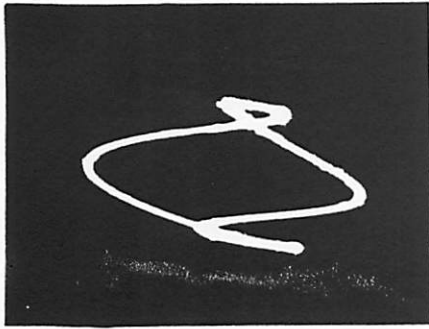


(a)

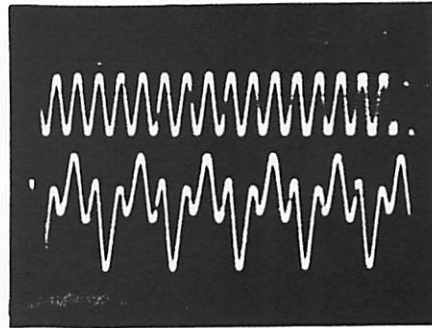


(b)

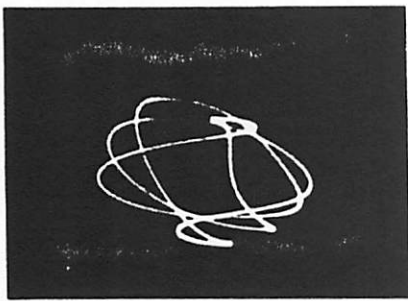
Figure 2



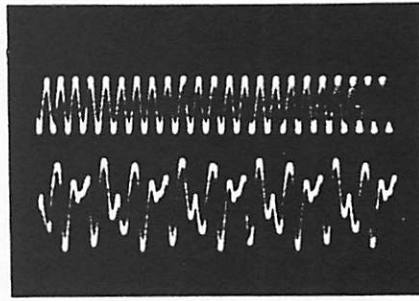
(a)



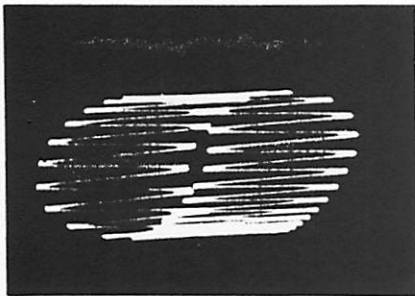
(b)



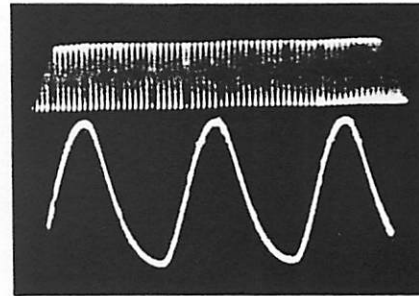
(c)



(d)



(e)



(f)

Figure 3

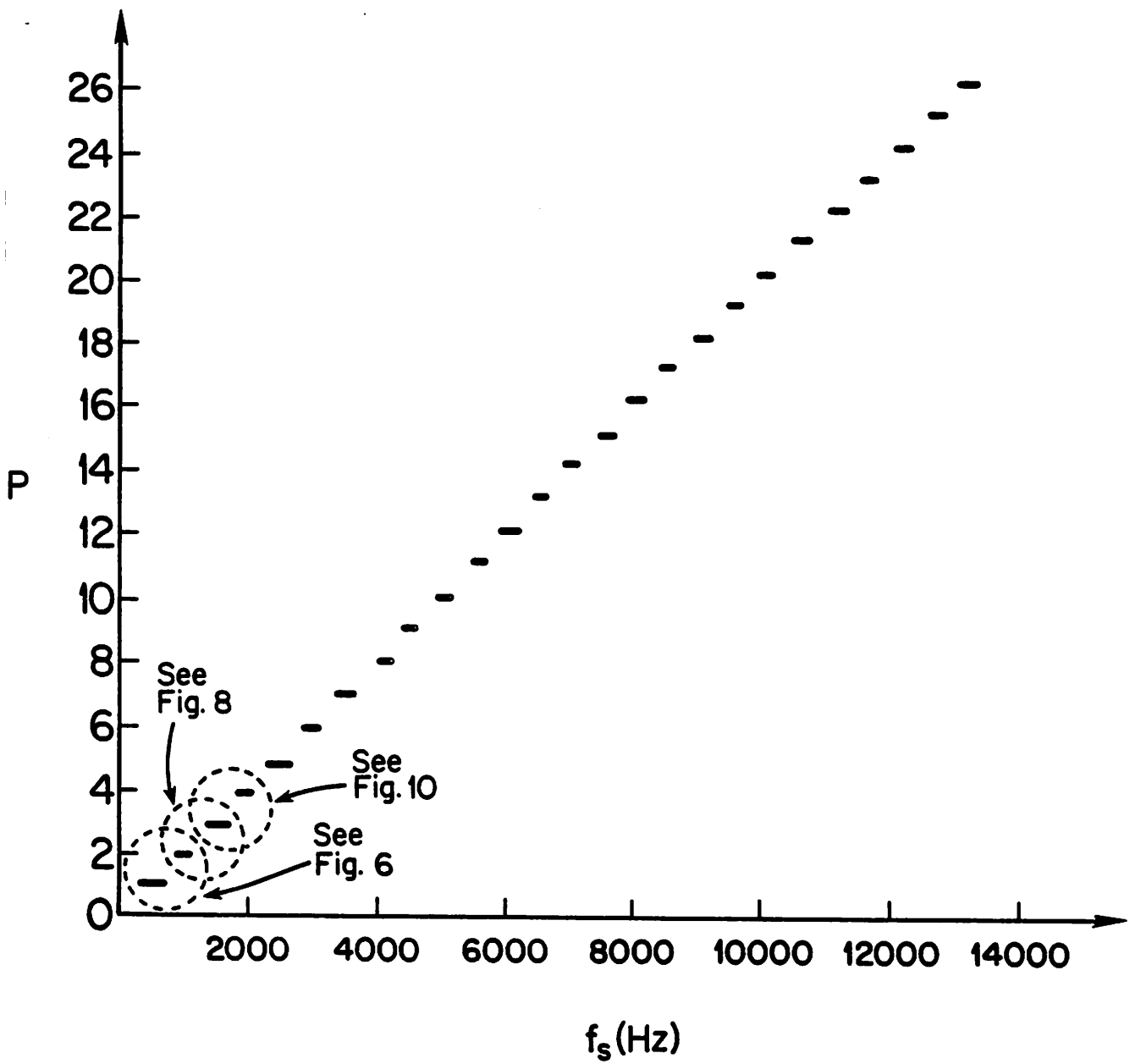
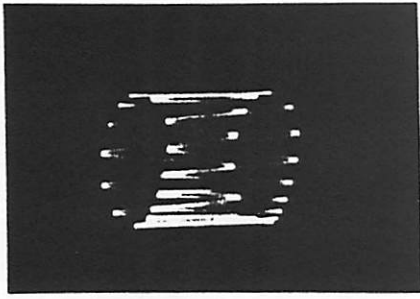
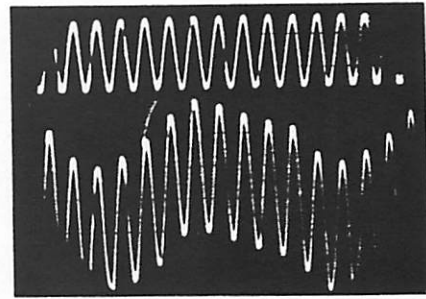


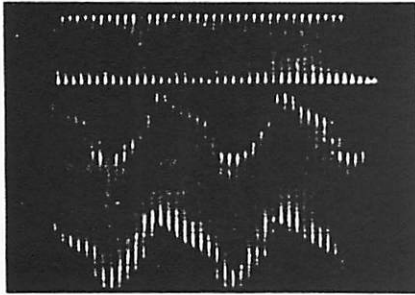
Figure 4



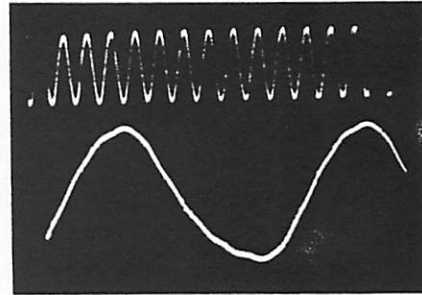
(a)



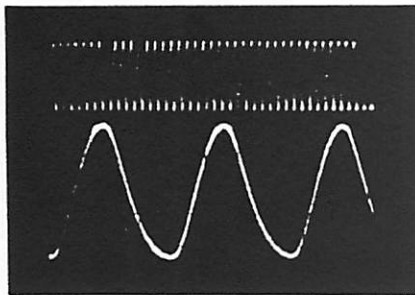
(e)



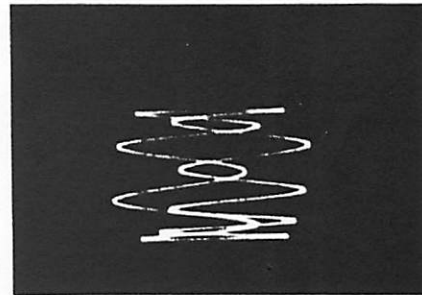
(b)



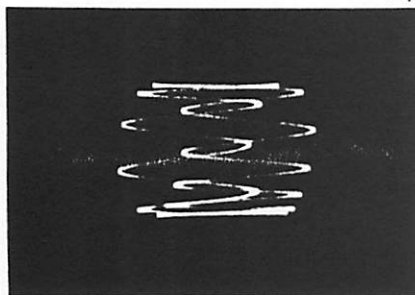
(f)



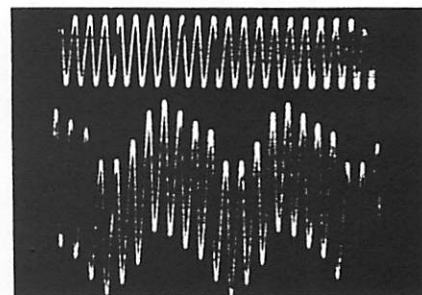
(c)



(g)



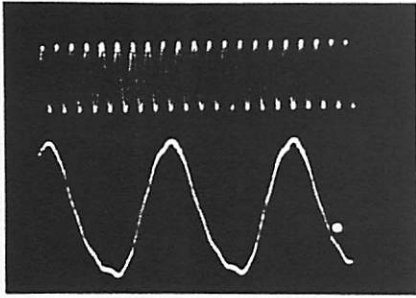
(d)



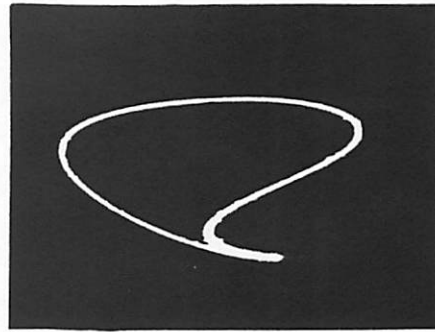
(h)

Figure

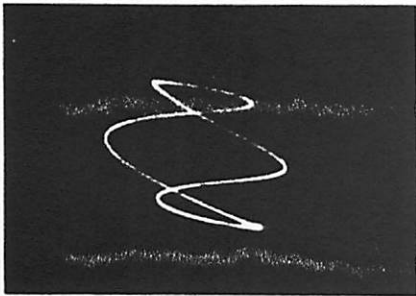
Figure 5



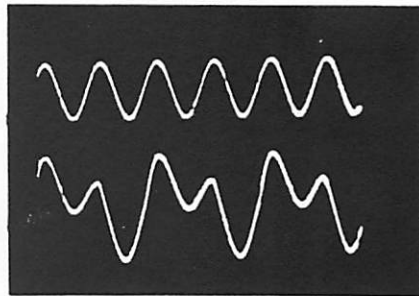
(i)



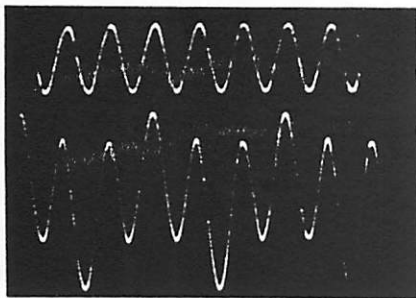
(m)



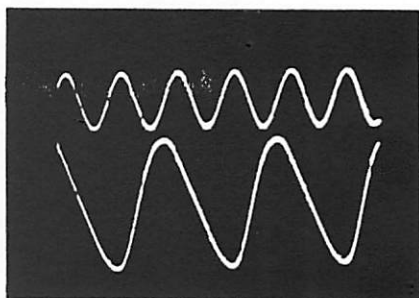
(j)



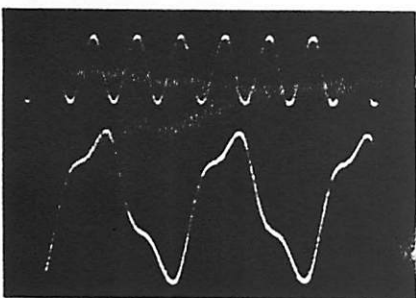
(n)



(k)



(o)



(l)

Figure 5(cont.)

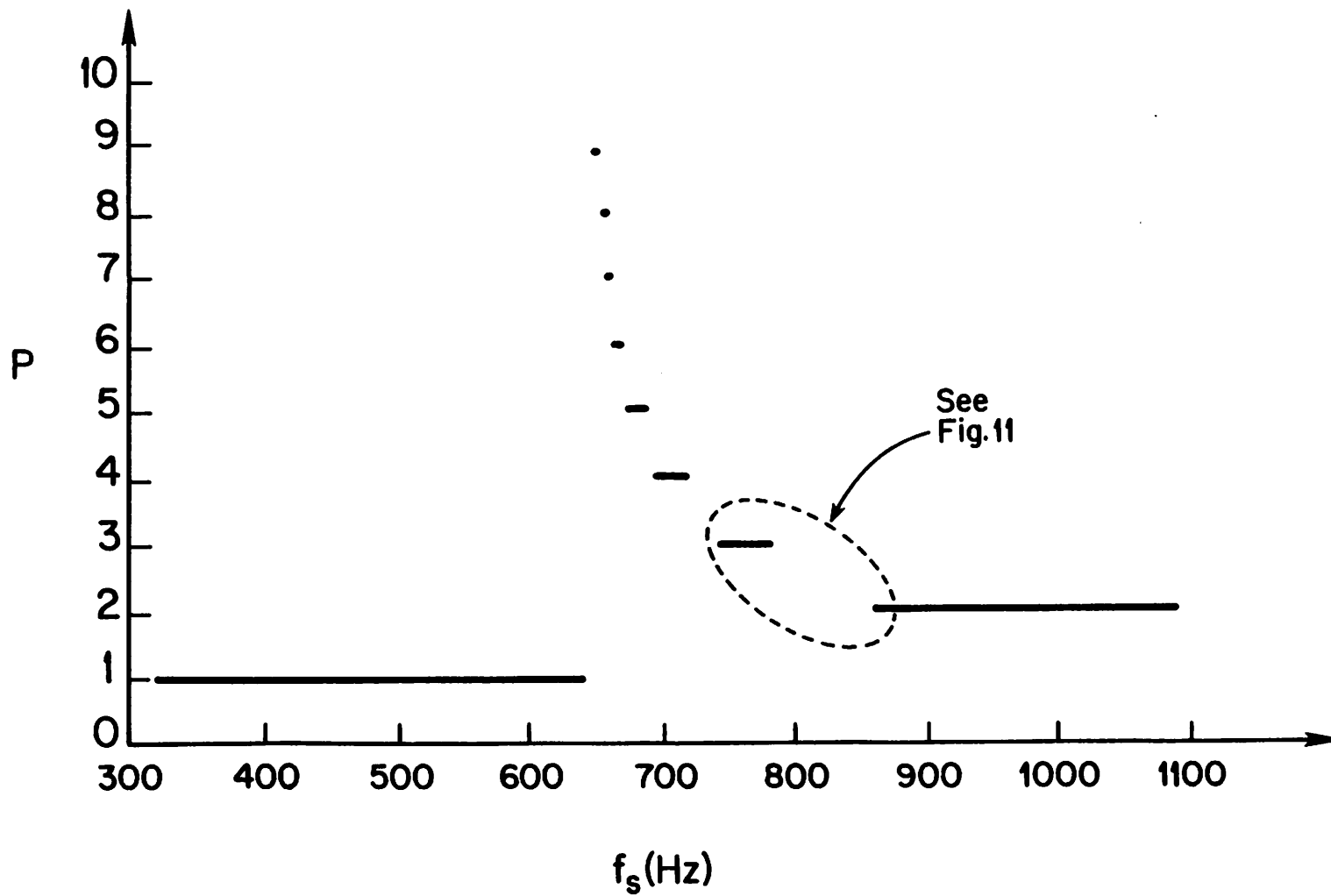
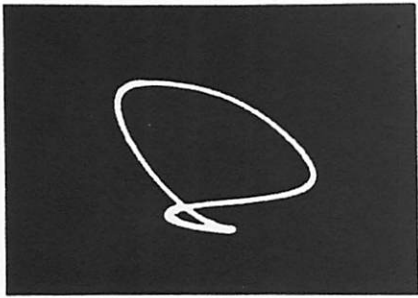
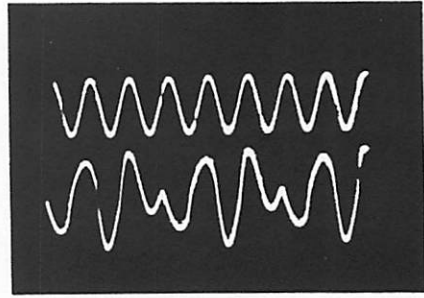


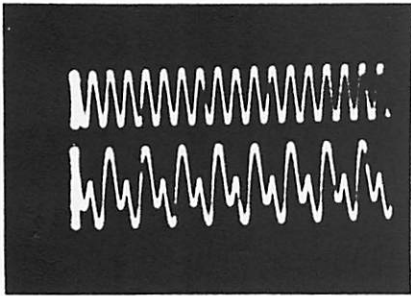
Figure 6



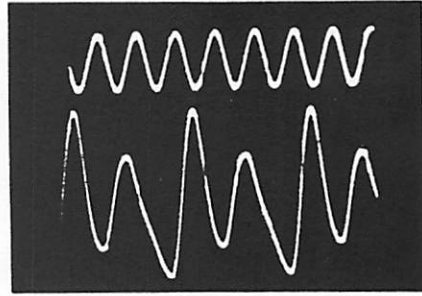
(a)



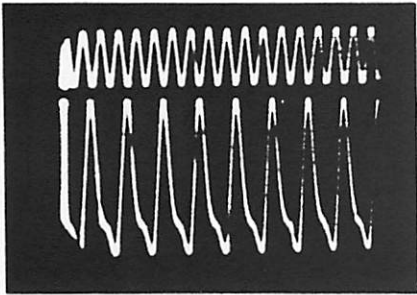
(e)



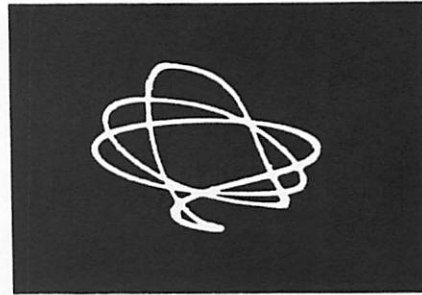
(b)



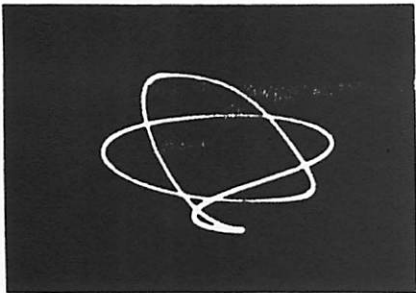
(f)



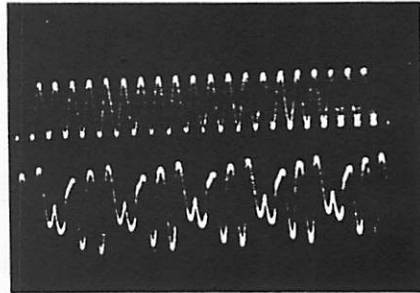
(c)



(g)

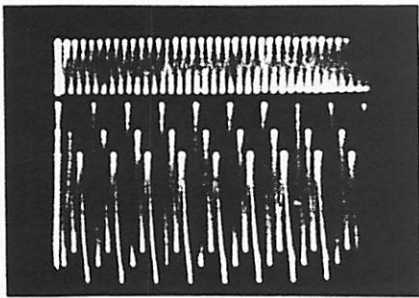


(d)

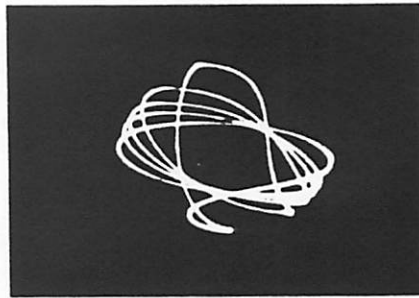


(h)

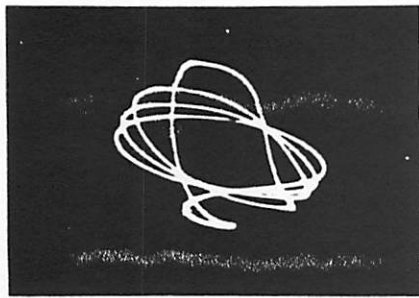
Figure 7



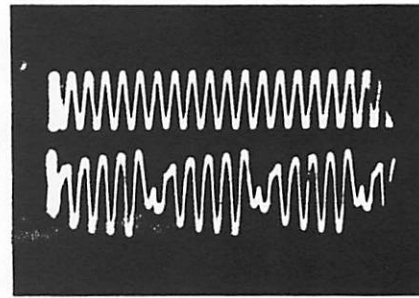
(i)



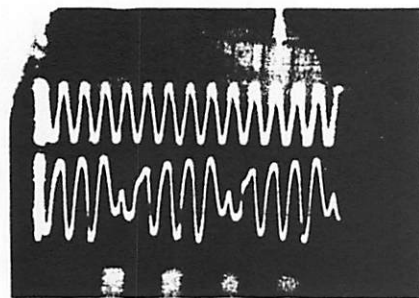
(m)



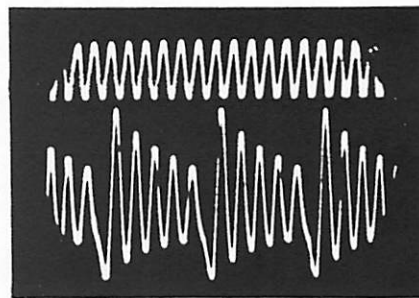
(j)



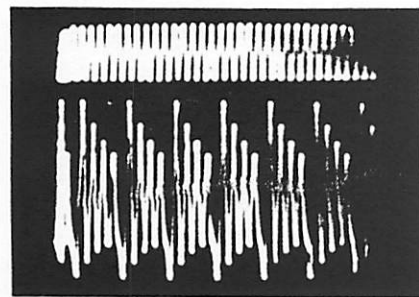
(n)



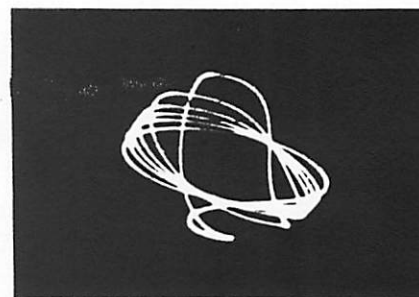
(k)



(o)

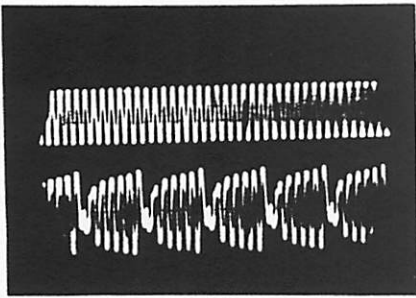


(l)

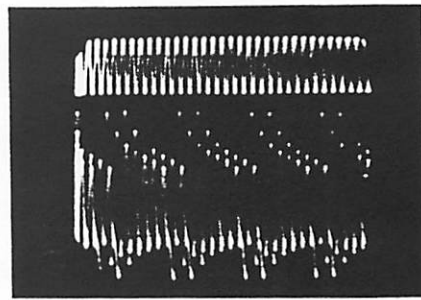


(p)

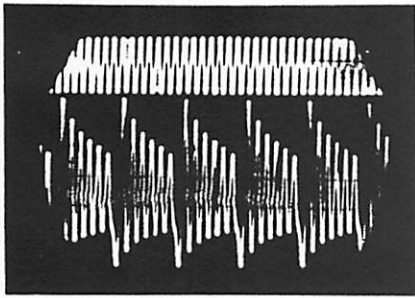
Figure 7 (cont.)



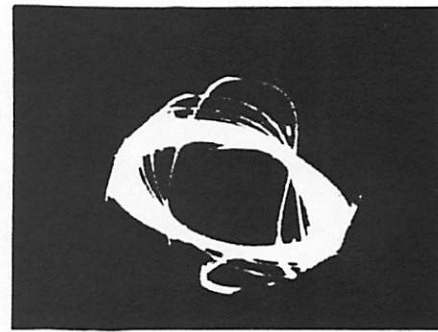
(q)



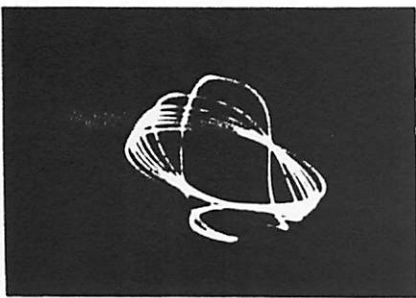
(u)



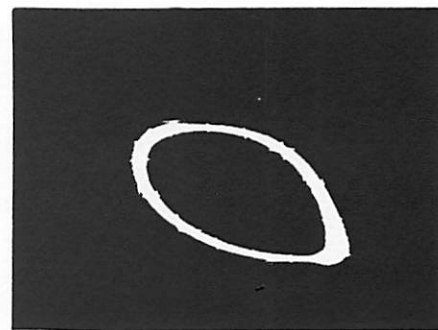
(r)



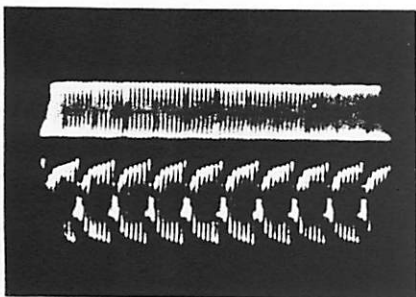
(v)



(s)



(w)



(t)

Figure 7(cont.)

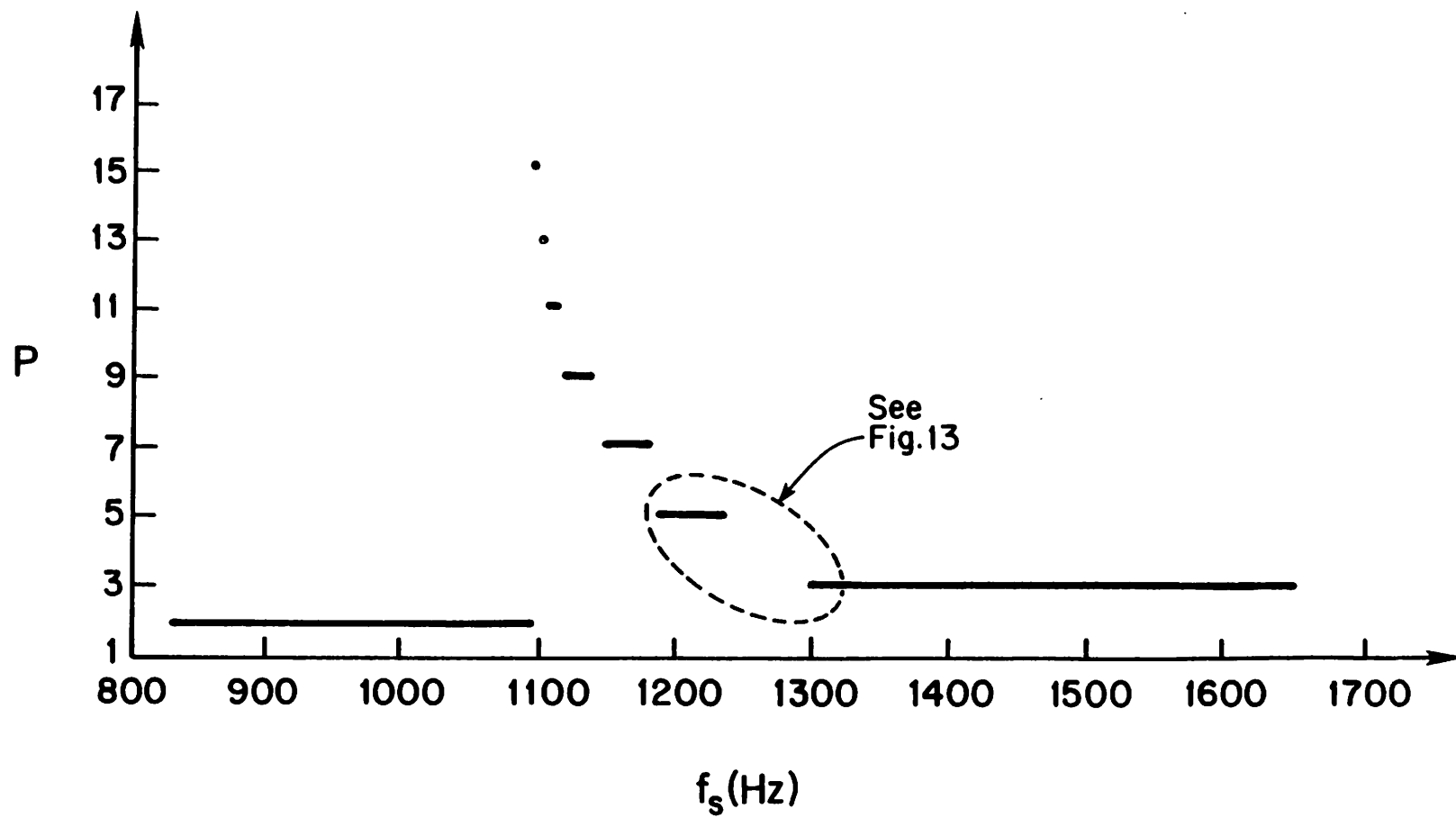
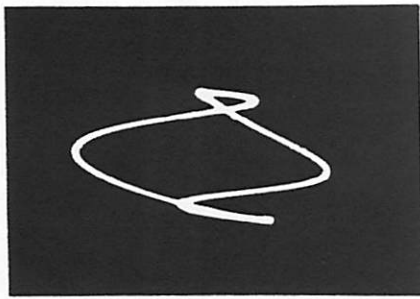
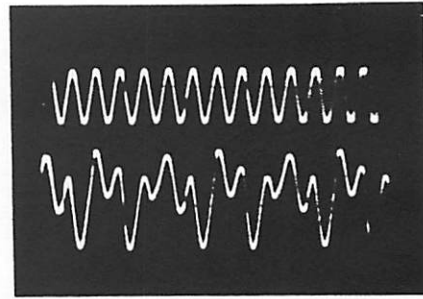


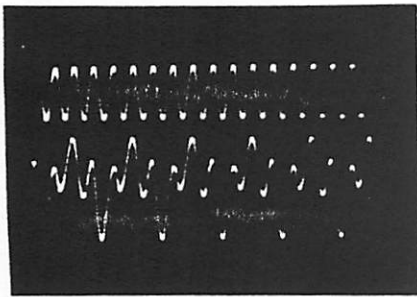
Figure 8



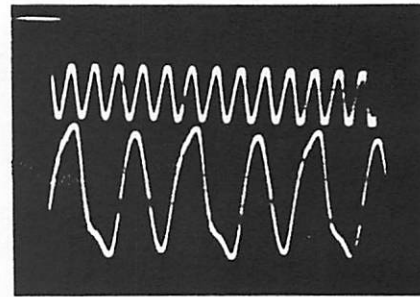
(a)



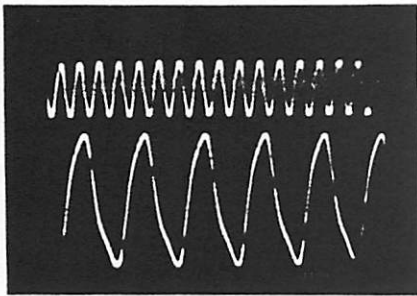
(e)



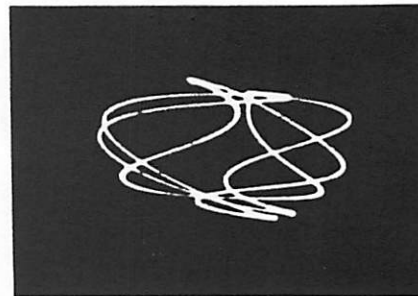
(b)



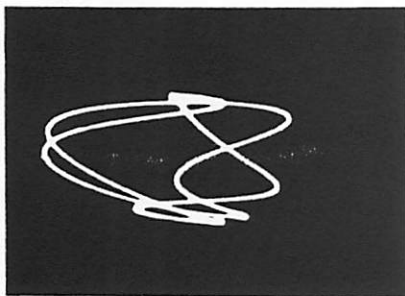
(f)



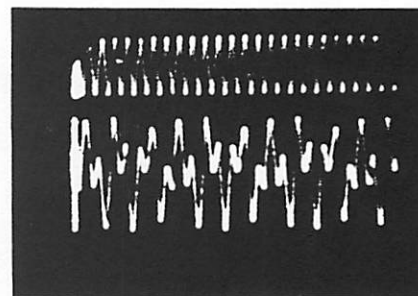
(c)



(g)

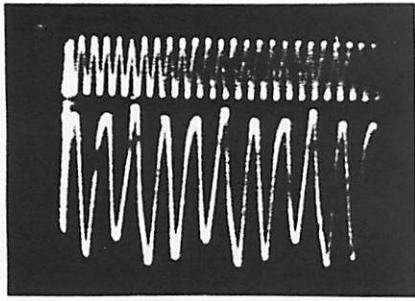


(d)

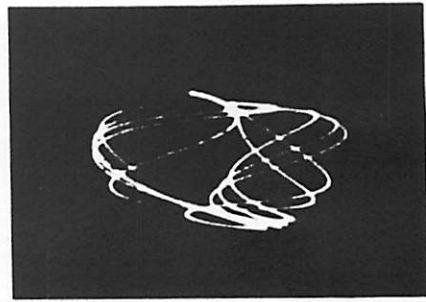


(h)

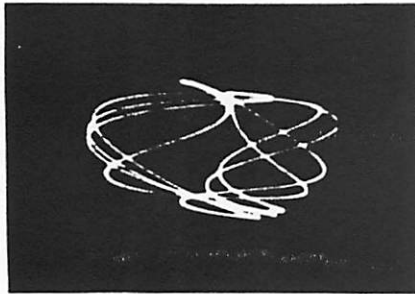
Figure 9



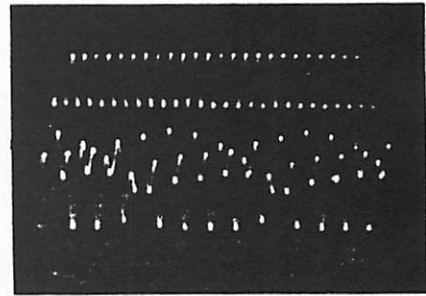
(i)



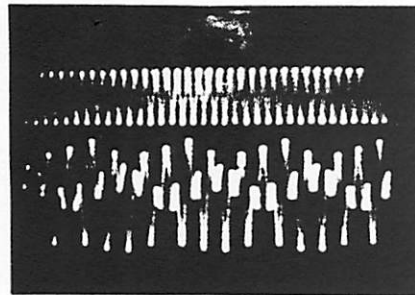
(m)



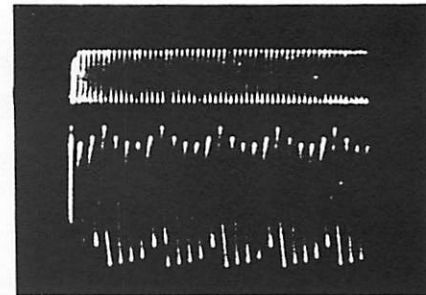
(j)



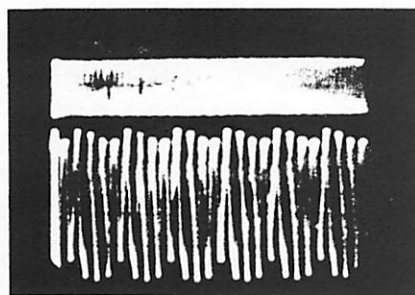
(n)



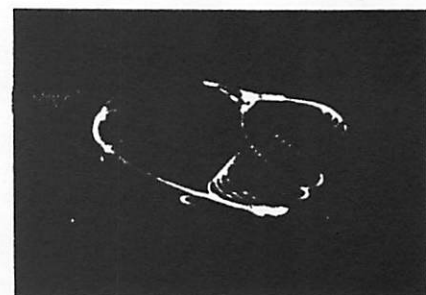
(k)



(o)

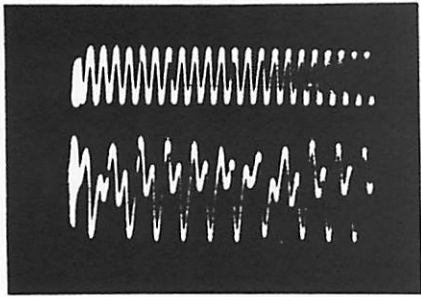


(l)

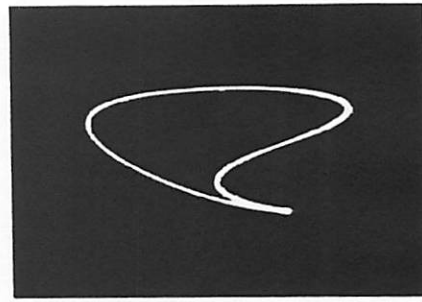


(p)

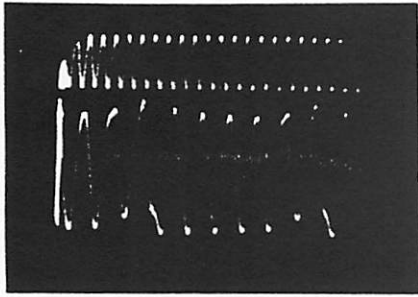
Figure 9(cont.)



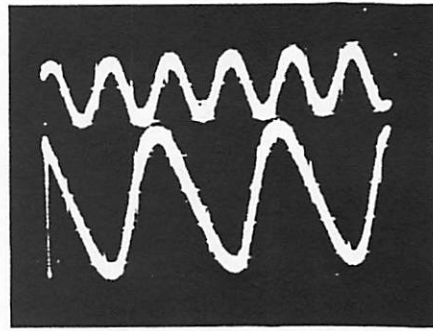
(q)



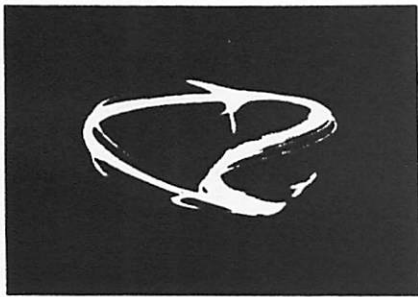
(u)



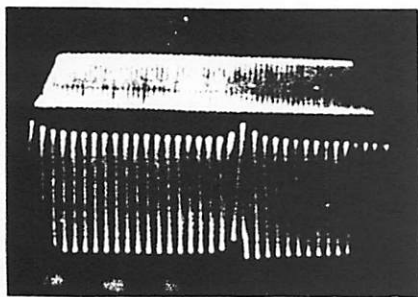
(r)



(v)



(s)



(t)

Figure 9 (cont.)

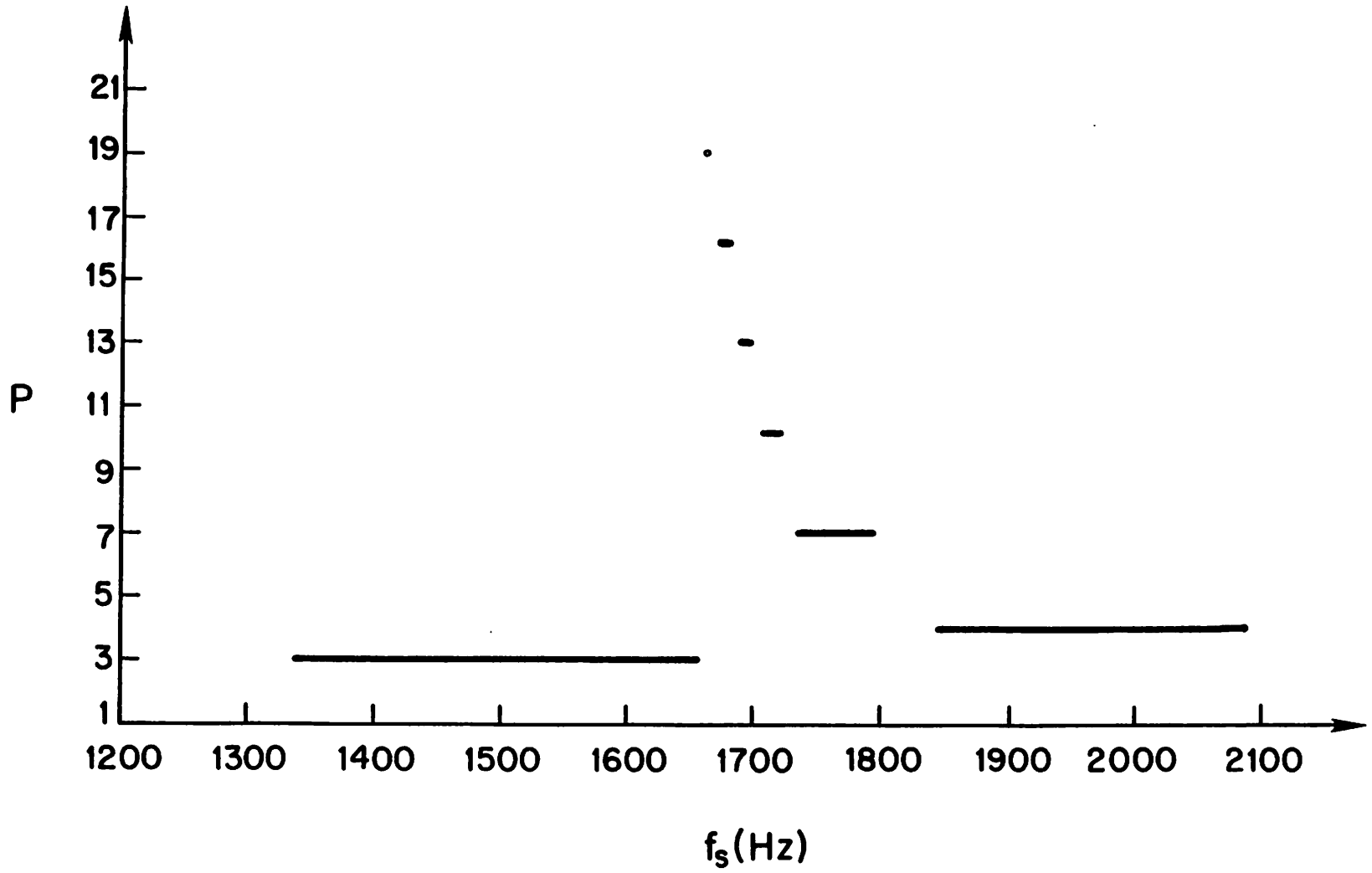


Figure 10

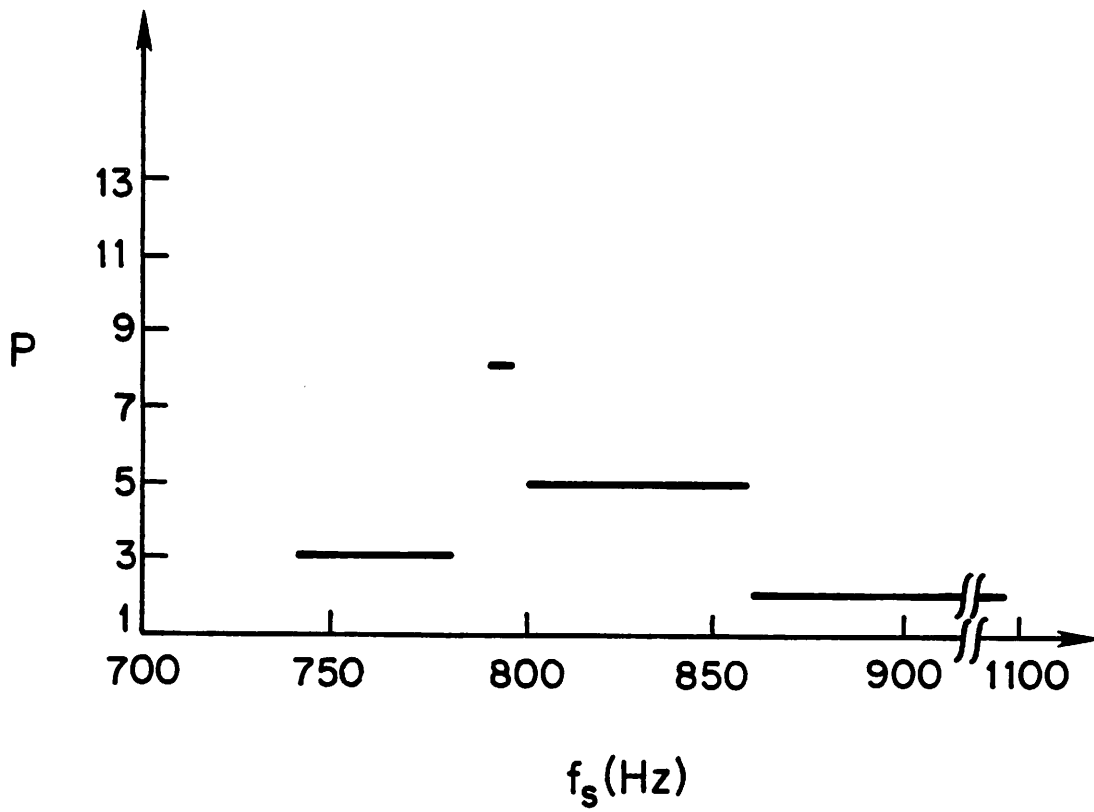
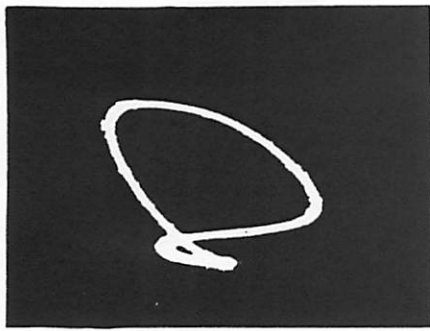
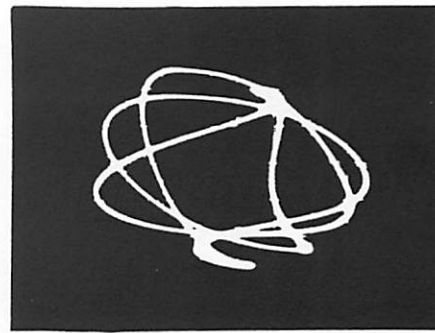


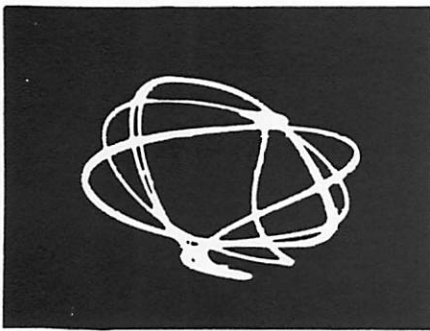
Figure 11



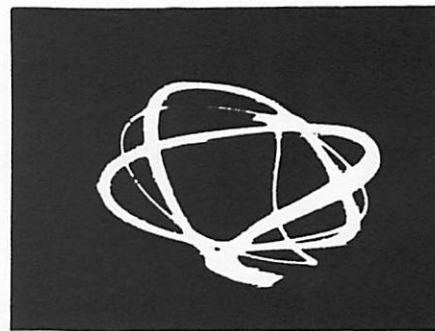
(a)



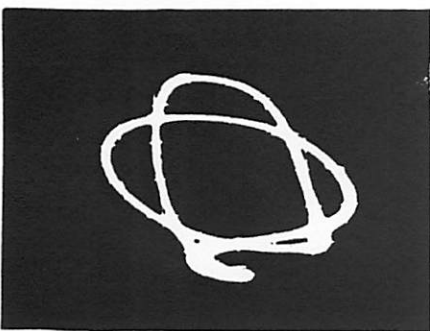
(b)



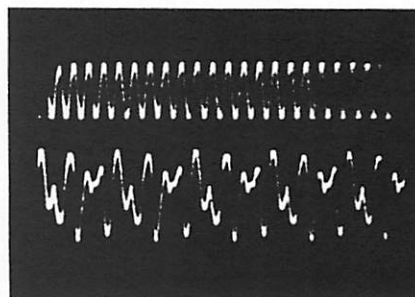
(c)



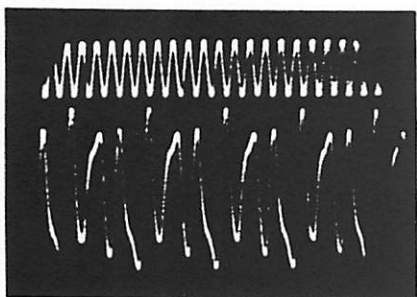
(d)



(e)



(f)



(g)

Figure 12

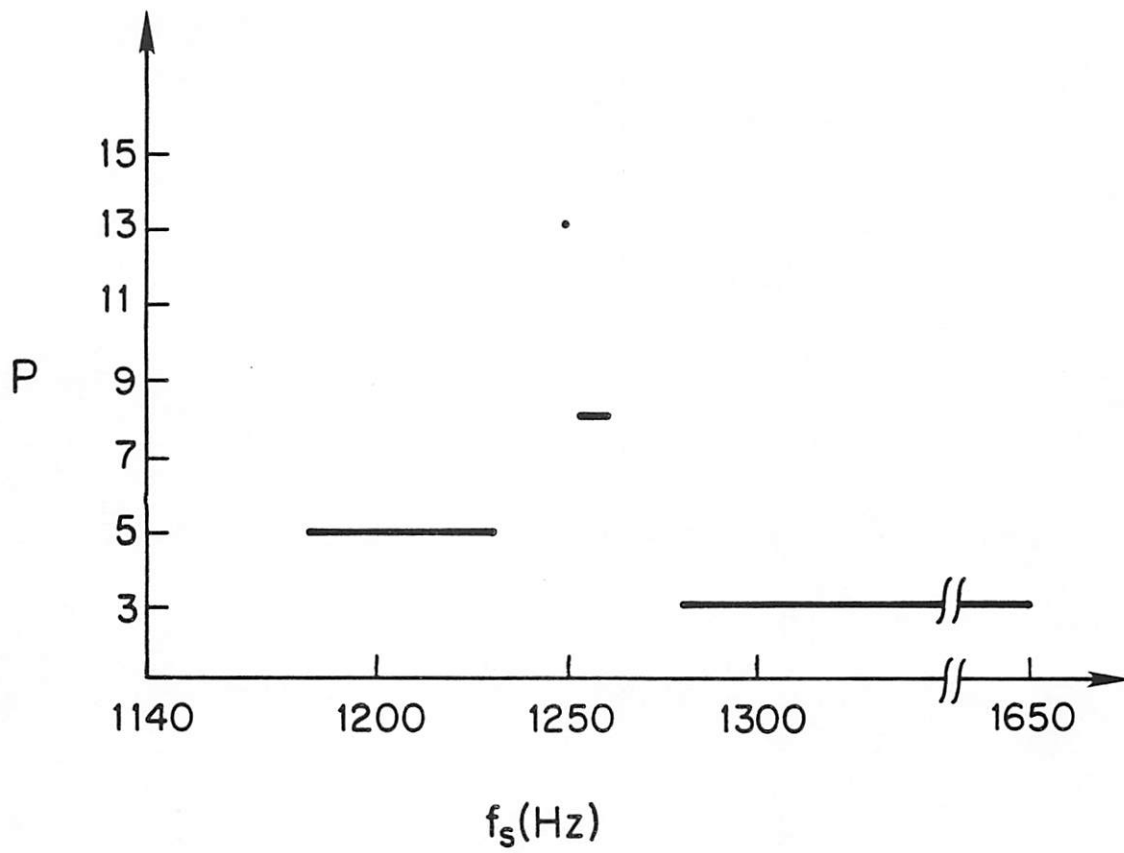
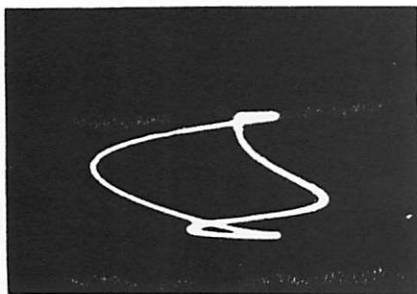
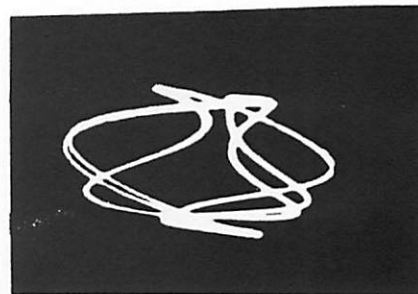


Figure 13



(a)



(b)

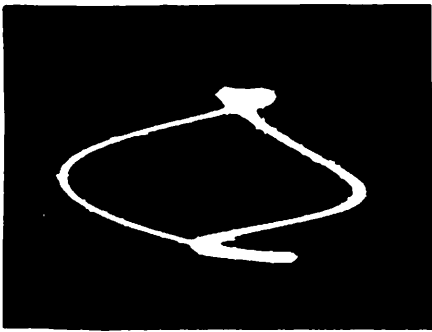


(c)

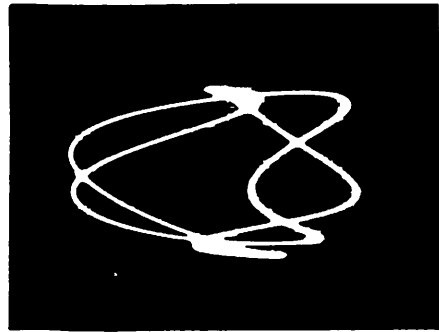


(d)

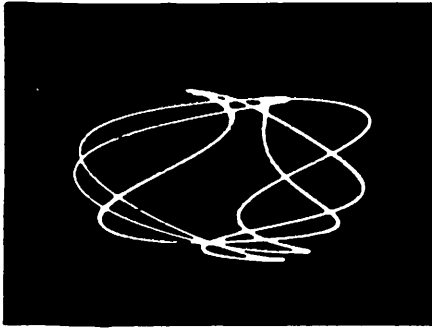
Figure 14



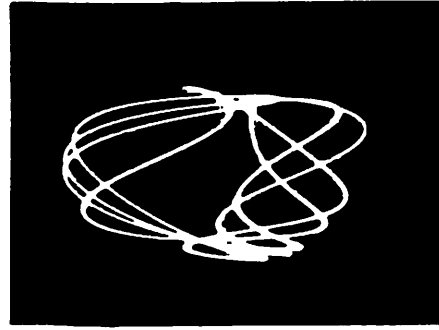
(a)



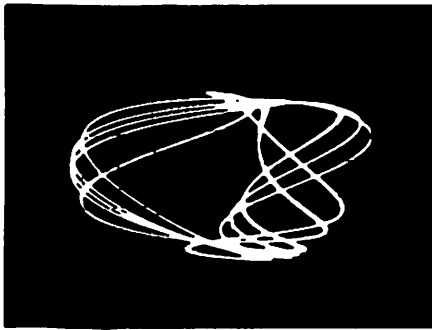
(b)



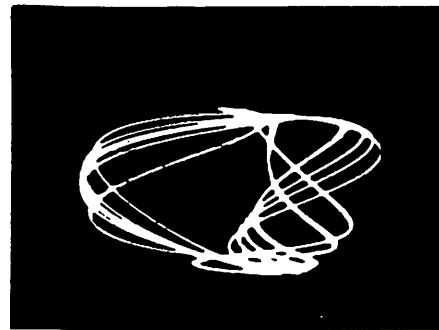
(c)



(d)



(e)



(f)



(g)



(h)

Figure 15